Iranian Journal of Science (2023) 47:695–705
https://doi.org/10.1007/s40995-023-01451-5

RESEARCH PAPER

Histopathologic, Biochemical, and Biodistribution Studies of Orally Administrated Silica and Magnesium Oxide Nanoparticles in Rats

Samira Ghorbani[1] · Hamdallah Moshtaghi[2] · Seyed Shahram Shekarforoush[3] · Hamid Reza Gheisari[3] · Fatemeh Sedaghati[4] · Saeid Nazifi[5] · Nasrollah Ahmadi[6]

Received: 19 July 2022 / Accepted: 10 March 2023 / Published online: 11 April 2023

Abstract

Nanoparticles (NPs) are being used in several industries worldwide and can introduce into the human body through different exposure routes, including inhalation, oral administration, intravenous injection, and intramuscular or transdermal delivery. The present in vivo study aimed to evaluate the acute oral toxicological effects of silica (SiO_2) and magnesium oxide (MgO) NPs in rats by using histological, biochemical, and biodistribution parameters. The results revealed that acute exposure to higher doses of these NPs produced a significant decrease ($p < 0.05$) in alanine aminotransferase, alkaline phosphatase serum levels lactate dehydrogenase, and aspartate aminotransferase. Mild congestion, non-zonal hepatocellular swelling and degeneration, and apoptotic cells with significant pyknotic or shrunken nuclei were found in the liver of the treated rats at 2000 mg/kg of the MgO NPs. Moreover, under the microscopic examination, focal hepatocellular degeneration and necrosis, accumulation of mononuclear inflammatory cells within the necrotic area and in the portal tract, and severe central vein and sinusoidal congestion and focal edematous fluids in the hepatic parenchyma were observed in the livers of the treated rats with 2000 mg/kg of SiO_2 NPs. Moreover, MgO NPs exhibited higher liver and kidney accumulation than SiO_2 NPs. In conclusion, these NPs at a high concentration could have toxicological effects on rats' liver and kidney tissues. However, further studies require examining the safety and the other possible toxic effects of these NPs before entering the consumer market.

Keywords Biodistribution · Magnesium oxide nanoparticles · Nanotoxicity · Silica nanoparticle · Wistar rats

1 Introduction

Nanomaterials (NMs) are globally produced in large quantities due to their broad potential applications in industrial processes agriculture, biology, biomedical research, diagnostic imaging, electronics, sunscreens, cosmetics, personal care, food products, and safety, antibiotic products, therapeutic preparations, and drug and gene delivery (Scenihr 2007; Sahoo et al. 2007; Zhang et al. 2012; Hassankhani et al. 2015).

The utilization of NPs in various fields has increased throughout the world exponentially. However, human and environmental exposure to NPs may, in turn, lead to significant adverse effects on human health which are inevitable (Mangalampalli et al. 2017).

Among the known nanoparticles, magnesium oxide (MgO) NPs and silica (SiO_2) NPs have attracted wide scientific interest due to their ease of synthesis, chemical stability, unique properties, and extensive

Hamid Reza Gheisari: Deceased

✉ Samira Ghorbani
s.ghorbani@ardakan.ac.ir

1 Department of Food Hygiene and Quality Control, Faculty of Veterinary Medicine, Ardakan University, Yazd, Iran

2 Department of Food Hygiene and Quality Control, Faculty of Veterinary Medicine, Shahrekord University, Shahrekord 34141, Iran

3 Department of Food Hygiene and Public Health, School of Veterinary Medicine, Shiraz University, Shiraz, Iran

4 Department of Chemistry, Estahban High Education Center, Estahban, Iran

5 Department of Clinical Pathology, School of Veterinary Medicine, Shiraz University, Shiraz, Iran

6 Department of Pathobiology, School of Veterinary Medicine, Shiraz University, Shiraz, Iran

applications in various fields (Nishimori et al. 2009; Yu et al. 2012).

Amorphous SiO_2 NPs, a typical kind of NMs, have been widely applied in cosmetics, medicine, and drug delivery systems (Morishita et al. 2012). For several decades, SiO_2 NPs have been commonly used in food products within the EU as a food additive (E551), anticaking agent, and carrier of flavors (van der Zande et al. 2014; Park et al. 2020). MgO NPs have attracted broad scientific interest due to their ease of synthesis, chemical stability, unique properties, and wide applications in various areas such as industry, medicine, and foodstuff (Krishnamoorthy et al. 2012; Ghobadian et al. 2017). Also, these NPs have been applied to relieve heartburn, sore stomach, and acid indigestion as an antiacid, detoxifying agent, and bone regeneration (Martinez-Boubeta et al. 2010; Gelli et al. 2015; Mazaheri et al. 2019).

The unique physicochemical properties of NPs, including their size, shape, and surface area, are considered critical factors in evaluating their nano-toxicity (Kim et al. 2014). For example, as a function of their size, they are responsible for their increased cell permeability and quantum effects (Hochella et al. 2008; Ivask et al. 2015). Many studies have demonstrated that different types of NPs have toxic effects on various tissues, including the liver, kidney, lung, and spleen. With the increasing production and applications of the NPs in human life, the exposure to these NPs and concerns about their biosafety aspect have drawn more attention (Fu et al. 2012; Hassankhani et al. 2015). Silica is used as an anti-caking agent to improve the flow property of powered components and as a carrier for flavors or active ingredients in the food. Along with the rapid development of nanotechnology, the sizes of silica fall into the nanoscale, thereby raising concerns about the potential toxicity of nano-sized silica materials (Go et al. 2017).

It is possible that these NPs would be administered into the human body through different exposure pathways, such as inhalation, oral administration, intravenous injection, and intramuscular and transdermal delivery. Therefore, it is essential to ensure their safety and obtain the information necessary for designing safe NMs or assessing the toxic effects of the NPs (Fu et al. 2013; Cho et al. 2009). In vivo studies for the toxicological assessment of NPs are important because animal systems are extremely complicated and their interactions with biological systems could lead to novel immune responses, metabolism patterns, biodistribution, and clearance which provide useful information on likely health hazards evaluation in mankind (Fischer and Chan 2007). For these reasons, the present study was carried out to investigate the absorption, distribution, and oral toxicity of SiO_2 and MgO NPs in rats by using histological, biochemical, and biodistribution analysis. To provide experimental evidence for evaluating the toxicity of the NPs, their quantitative distribution of the NPs content was assessed using inductively coupled plasma-optical emission spectrometry (ICP-OES) and atomic absorption spectroscopy (AAS) in the liver and kidney.

2 Materials and Methods

2.1 Synthesis of SiO_2 NPs

SiO_2 seeds with an ultra-small size were prepared by the injection of 10 µL tetraethyl orthosilicate (TEOS, 98% Sigma-Aldrich) into 1 mL deionized water under ultrasonication (280W, Sono-Swiss/SW3H) and allowed to proceed for 24 h under magnetic stirring in a water bath with a temperature of 45 °C. Subsequently, 5 µL of TEOS was added to each 1 ml of the original reaction solution every 24 h. Finally, after a total reaction time of 72 h, the reaction vessel was cooled at room temperature (Ding et al. 2016).

We used the modified Stober method for the synthesis of large-size SiO_2 NPs. In a typical synthesis, 90 mL ethanol (99%) was mixed with 10 mL of deionized water under magnetic stirring. Next, 1 mL of SiO_2 seed solution, 2 mL ammonia solution (28–30%), and 2.5 mL TEOS were added into the mixture separately and stirred at room temperature for 24 h. Finally, the resulting particles were centrifuged and repeatedly washed with deionized water to remove any unreacted reagents and dried at 150 °C for 2 h (Ding et al. 2016).

2.2 Synthesis of MgO NPs

In a typical procedure, 25 mL of 1 M $MgCl_2{\cdot}6H_2O$ solution was prepared and poured into a beaker. A buret was used to deliver 25 mL of 1 M Na_2CO_3 solution into a container of $MgCl_2$ solution with a flow rate of about 10 mL/min to form white precipitation. Then, the autoclave (100-mL Teflon lined autoclave reactor) was filled up to 2/3 of the total volume with the reaction mixture, sealed, and heated in the oven at 80 °C for 2 h. After cooling, the precipitate was separated from the solution by centrifugation at 5000 RPM for 15 min and washed with deionized water three times. The precipitate yielded MgO nanostructures at an optimal calcination temperature of 500 °C in a furnace for 6 h with a temperature ramping rate of 2 °C/min (Purwajanti et al. 2015).

2.3 Characterization of the Synthesized NPs

Scanning electron microscopy and transmission electron microscopy (SEM and TEM) were used to characterize the NPs to understand the size, shape, and particle size distribution. Also, X-ray diffraction (XRD) was applied to determine crystalline character, crystallite size, crystal structures, and lattice constants of the NPs. SEM experiments were carried out at an accelerating voltage of 20 kV on a scanning electron microscope (SEM, Zeiss, SUPRA VP 40). The samples were examined by a TEM model LEO LIBRA at an accelerating voltage of 120 k. X-ray powder diffractometer (Cu Kα radiation, $k = 0.15406$ nm) between 5° and 100° was used. To estimate the range and average size of NPs, we used ImageJ software (Wayne Rasband, NIH, USA).

2.4 Experimental Animals

Twenty-four female Wistar rats weighing 190 ± 10 g were obtained from the laboratory animal center belonging to Shiraz University of Medical Sciences, Shiraz, Iran. They were acclimated in the controlled conditions (temperature: 23 ± 2 °C, relative humidity: 60 ± 5%, and exposure to a 12-h light/dark cycle) with free access to diet and water. In the present experimental study, all animal handling procedures were carried under the approval of the State Committee on Animal Ethics, Shiraz University, Shiraz, Iran (ethical approved number 1395/931113105).

An acute oral toxicity study was conducted according to the OECD Guidelines for the Testing Chemicals (OECD No. 420, 2001). As per the test guideline, the observation period is 14 days. It consisted of a sighting study and the main study. In the sighting study, the single female rat was administered 5, 50, 300, and 2000 mg/kg BW doses sequentially. The main study was conducted with a single acute dose of 2000 mg/kg. Based on the preliminary data, the LD50 of MgO and SiO_2 NPs in rats was determined to be higher than 2000 mg/kg. After a week of acclimatization, the animals were randomly divided into three groups ($n = 8$) as follows: The first group served as a control; these animals received distilled water. Group 2 was administered with 2000 mg/kg body weight MgO NPs, and Group 3 was treated with 2000 mg/kg body weight SiO_2 NPs. The suspension of 2000 mg/kg of MgO and SiO_2 nanoparticles was administered once using oral gavage.

2.5 Biochemical and Histopathological Analysis

At day 14 of the treatment, the overnight-fasted rats were anesthetized and bled from the heart for the serum collections. The serum was separated by centrifugation at $3000 \times g$ for 15 min and kept at − 70 °C for subsequent biochemical analysis. The serum was analyzed for total protein by the biuret method (Commercial kit; Pars Azmoon, Tehran, Iran) and albumin by the bromocresol green method (Commercial kit; Pars Azmoon, Tehran, Iran). Biochemical analyses, including cholesterol, lactate dehydrogenase (LDH), alanine aminotransferase (ALT), aspartate aminotransferase (AST), alkaline phosphatase (ALP), blood urea nitrogen (BUN), creatinine (Cr), phosphorus, calcium, glucose, and triglyceride, were done using a Biochemical Autoanalyzer (Alpha Classic Model, Sanjesh Diagnostic Company, Iran).

After bleeding, the animals were killed by CO_2 gas asphyxiation. The liver, kidney, heart, lung, and spleen were initially excised and rinsed in chilled saline solution. Immediately, a small piece of these tissues were fixed in 10% neutral buffered formalin for 24–48 h at room temperature. After complete fixation, the specimens were dehydrated in the graded alcohols and embedded in paraffin blocks, sectioned into 5–6 μm in thickness, and finally, stained with hematoxylin–eosin staining (H&E). The prepared slides were observed using a light microscope for the histopathological assessments.

2.6 The Measurement of the Amount of Si^{+4} and Mg^{+2} in the Tissues

To assess the distribution and accumulation of Si^{+4} and Mg^{+2}, they were analyzed in the liver and kidney of the treated rats. The tissue samples were weighed, digested in concentrated nitric acid and perchloric acid mixture (70:30), and heated at 80–90 °C until the solutions were colorless and transparent. The Si^{+4} and Mg^{+2} contents were analyzed using ICP-OES (VARIAN VISTA-MPX, US) and an atomic absorption spectrophotometer (ZEEnit 700 P, Analytik Jena, Germany), respectively.

2.7 Statistical Analysis

The data were analyzed using SPSS version 20 (SPSS Inc., Chicago, IL, USA). All results were expressed as Mean ± SD. The analysis of variance was used to determine significant differences among the treatments and the control groups. Duncan's post hoc test was applied to compare means when the effect was substantial. $p \leq 0.05$ was considered as the level of significance.

3 Results

3.1 Characterization of the Synthesized Nanostructures

TEM and SEM images showed that SiO_2 NPs were fairly uniform spherical particles with an average size of 90 nm

(the range size, 90–160 nm) (Figs. 1a, b, and 2). Also, no diffraction peaks were appeared on the XRD pattern of SiO_2 NPs (Fig. 3), except a broad reflection at $2\theta = 13°–30°$, suggesting an amorphous state of existing SiO_2 NPs.

The TEM and SEM images showed that MgO NPs were polyhedral with an average particle size of 50 nm (the range size, 40–90 nm) (Figs. 4a, b, and 5). On the XRD pattern of MgO NPs, as shown in Fig. 6, the diffraction peaks were (1 1 1), (2 0 0), (2 2 0), (3 1 1), and (2 2 2), respectively, matched with the cubic structure of MgO, which are in line with the standard and the findings reported by other studies (Dhal et al. 2015; Dummer et al. 2016). Diffraction peaks can be indexed in cubic structure space group Fm-3m (225) (ICSD collection code064930 Remark from ICSD/CSD REM M PDF 45-946) with unit cell parameter $a = 4.2$ Å. No characteristic peaks of other phases could be detected, which indicates a high purity of the obtained MgO materials.

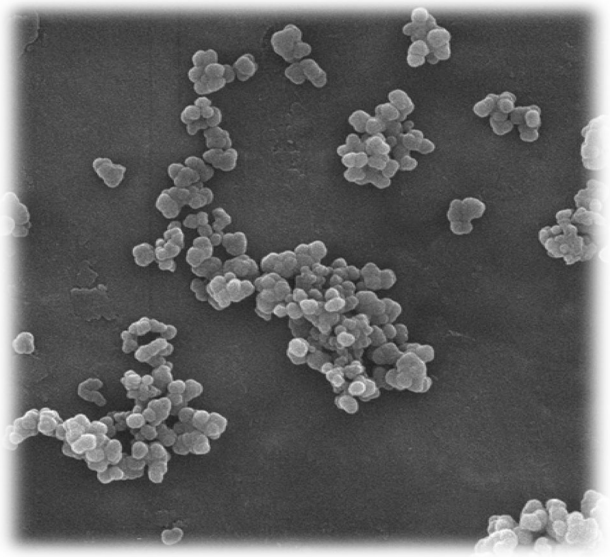

Fig. 2 The characterization of synthesized SiO_2 NPs. Scanning electron microscopy (SEM)

3.2 Serum Biochemical Analysis

The serum biochemical analysis of 2000 mg/kg SiO_2- and MgO NPs-treated rats revealed no significant difference in triglyceride and cholesterol between the control and the treated groups (Table 1). Treatment with 2000 mg/kg MgO NPs decreased serum glucose level compared to the control group, while with 2000 mg/kg of SiO_2 NPs, conversely, the serum glucose level increased. The 2000 mg/kg MgO doses and SiO_2 NPs significantly decreased the serum calcium level ($p < 0.05$). Also, treatment with doses of 2000 mg/kg SiO_2 NPs significantly reduced the phosphorus concentration in the serum ($p < 0.05$). The serum albumin, creatinine, and protein concentrations did not show any significant difference between the control and the treated groups.

As shown in Table 1, the AST, ALP, and ALT levels were significantly reduced in the serum of 2000 mg/kg MgO NPs-treated rats ($p < 0.05$). Serum ALT level was significantly ($p < 0.05$) decreased at the acute doses of 2000 mg/kg SiO_2 NPs, while AST and ALP activity level did not show any significant difference in the SiO_2 NPs-treated rats compared to the control group (Table 1). Also, there were a significant decrease and increase ($p < 0.05$) in the serum concentration of BUN in the treated rats with 2000 mg/kg of MgO and SiO_2 NPs compared to the control group, respectively (Table 1).

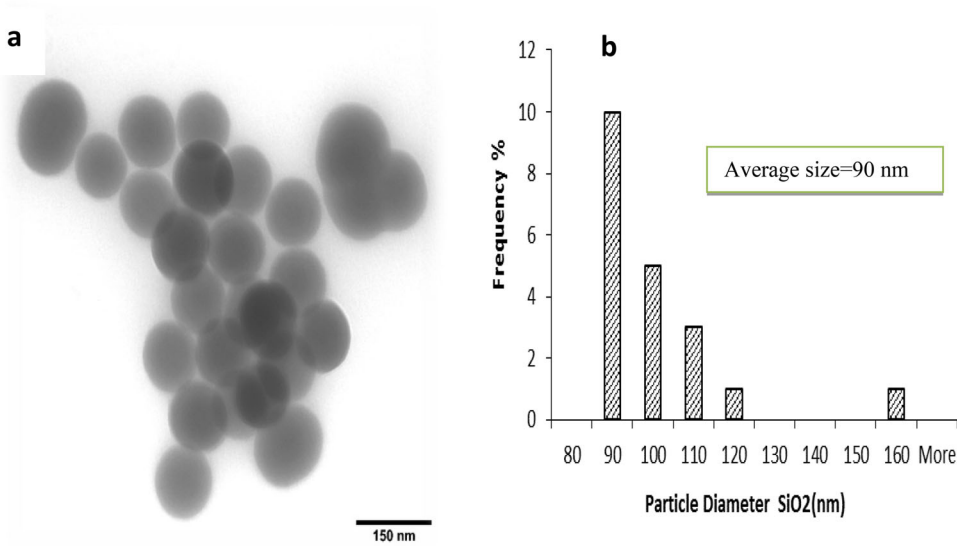

Fig. 1 The characterization of synthesized SiO_2 NPs. **a** Transmission electron microscopy (TEM); **b** size distribution histogram of SiO_2 NPs

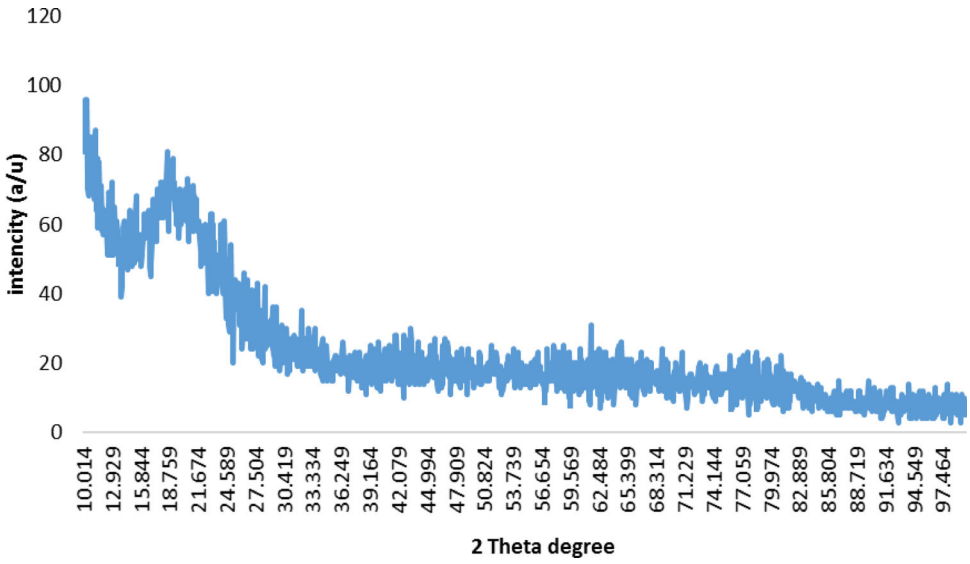

Fig. 3 X-ray diffraction profile of the synthesized SiO_2

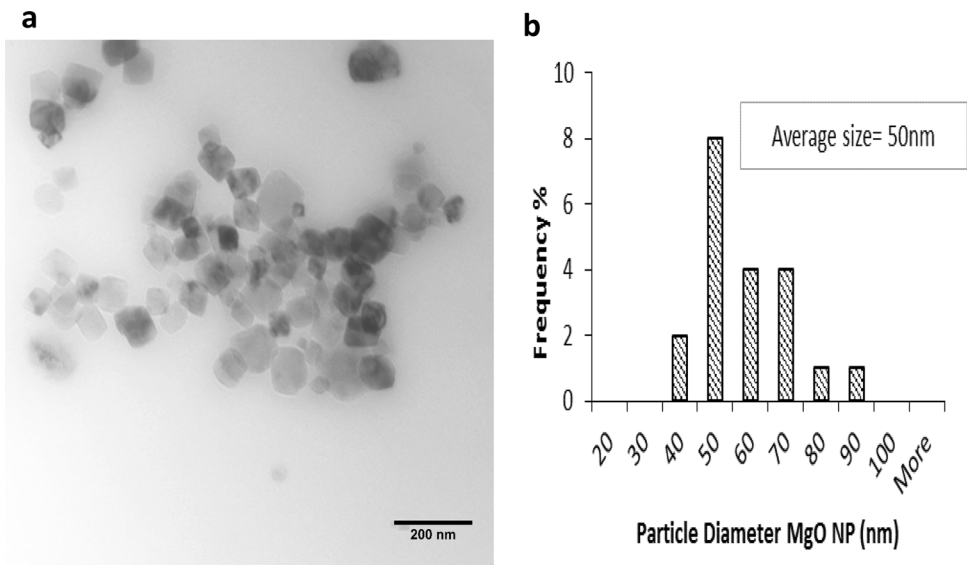

Fig. 4 The characterization of synthesized MgO NPs. **a** Transmission electron microscopy (TEM); **b** size distribution histogram of MgO NPs

3.3 Clinicopathological Analysis

In the present study, there was no mortality or signs of toxicity and discomfort (lethargy, nausea, vomiting or diarrhea) following the daily single oral administration of these NPs. All the rats survived at the end of the study period for 14 days. From the macroscopic point of view, no significant pathological changes were observed in all the organ systems of the control and the treated rats.

The histopathological analysis of the H&E-stained tissue sections of the heart, lung, and spleen revealed no microscopic abnormalities in both doses of these NPs in the control and treated rats. The H&E-stained tissue sections of the liver and kidney from the control group exhibited normal hepatic and renal histological architecture, respectively (Fig. 7a, d).

The histopathologic examination of the liver tissue sections in the 2000 mg/kg MgO NPs-treated rats revealed mild congestion, non-zonal hepatocellular swelling and degeneration, and individual cell necrosis with significant pyknotic nuclei and eosinophilic cytoplasm. No notable vacuolar appearance indicative of steatosis or any histologic evidence of inflammatory cell infiltrates, fibrosis, cell proliferation, cholestasis, etc., was observed in the liver parenchyma of the treated rats (Fig. 7b). The histopathologic changes in the kidneys of the 2000 mg/kg MgO NPs-treated rats consisted of mild congestion and hemorrhage, irregularly renal tubular epithelial cell swelling, and cytoplasmic alterations in the convoluted tubules and loops of Henle without any nuclear changes, interstitial inflammation, and/or proliferative changes (Fig. 7e).

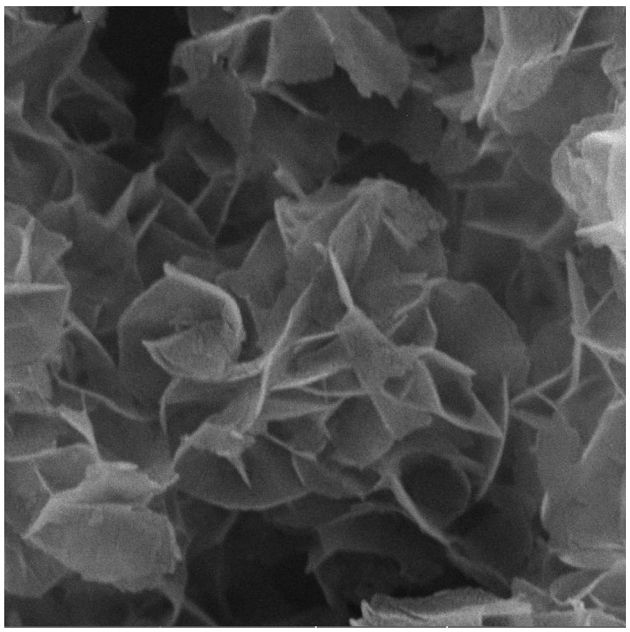

Fig. 5 The characterization of synthesized MgO NPs. Scanning electron microscopy (SEM)

In the liver of the 2000 mg/kg of SiO_2 NPs-treated rats with focal hepatocellular degeneration and necrosis, accumulation of mononuclear inflammatory cells within the necrotic area and in the portal tract, as well as severe central vein and sinusoidal congestion and focal edematous fluids in the hepatic parenchyma, was evident under the microscopic examination. Microscopically, minimal to mild random renal tubular epithelial cell swelling, degeneration, and vascular congestion were observed in the kidney tissue of the 2000 mg/kg SiO_2 NPs-treated rats (Fig. 7c, f).

3.4 Si^{+4} and Mg^{+2} Content Analysis

The biodistribution analysis of Si and Mg contents after acute oral exposure of the SiO_2 and MgO NPs with 2000 mg/kg doses was carried out in the liver and kidney tissues. The kidney and liver tissues of the treated rats with both doses of SiO_2 NPs showed a slight increase in the Si^{+4} content, but it was not statistically significant compared to the control group (Fig. 8). In the liver and kidney, the Si^{+4} content in the 2000 mg/kg SiO_2 NPs-treated rats was 0.282 and 0.380 µg/g tissue, respectively.

A significant increase ($p < 0.05$) in the Mg^{+2} content was found in the liver and kidney of the 2000 mg/kg MgO NPs-treated rats compared to the control group (Fig. 9). The Mg^{+2} content of the liver and kidney tissues in the 2000 mg/kg MgO NPs-treated rats was 244.5 and 177.75 µg/g tissue, respectively.

4 Discussion

In the near future, nanotechnology will play an important part in the world's economy and in our everyday lives. In spite of the great prospects of nanotechnology, there are increasing worries that intentional or accidental human and environmental exposure to NPs may lead to significant toxic effects. The SiO_2 and MgO NPs have drawn considerable international attention because of their various applications in the medical healthcare, biomedical, pharmacological fields, and else (Mangalampalli et al. 2017; Yu et al. 2012). Thus, it is greatly imperative to evaluate their safety. Herein, the present experimental study describes the histopathological changes due to the oral administration of SiO_2 and MgO NPs in rats and their absorption, biodistribution, and serum biochemical analysis.

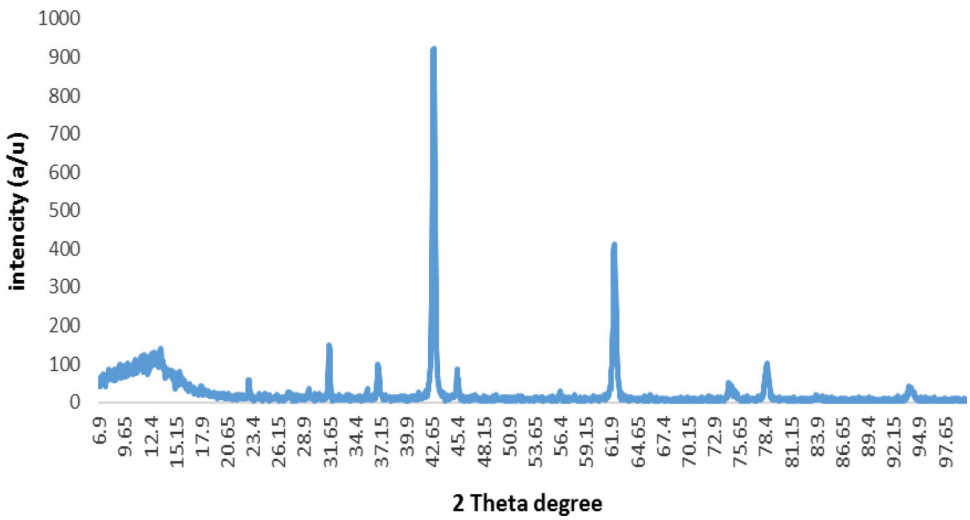

Fig. 6 X-ray diffraction profile of the synthesized MgO

Table 1 The effects of SiO_2 and MgO NPs on levels of the serum biochemical parameters of treated rats

Parameter	Control	MgO 2000 mg/kg	SiO_2 2000 mg/kg
Creatinine (mg/dL)	0.53 ± 0.02^{ab}	0.47 ± 0.02^{a}	0.51 ± 0.02^{ab}
Glucose (mg/dL)	110.8 ± 4.8^{b}	101.5 ± 3.3^{a}	128.2 ± 2.3^{c}
Cholesterol (mg/dL)	73.8 ± 6.6^{ab}	67.5 ± 4.9^{a}	70.1 ± 3.7^{ab}
Phosphorus (mg/dL)	5.3 ± 0.3^{a}	5.1 ± 0.5^{a}	3.9 ± 0.1^{b}
Protein (g/dL)	6.3 ± 0.1^{a}	6.1 ± 0.2^{a}	6.2 ± 0.1^{a}
Calcium (mg/dL)	9.76 ± 0.50^{c}	8.14 ± 0.39^{a}	8.50 ± 0.10^{ab}
Triglyceride(mg/dL)	157.8 ± 6.7^{ab}	149.4 ± 3.4^{a}	147.3 ± 6.8^{a}
Albumin (mg/dL)	3.70 ± 0.18^{ab}	3.40 ± 0.12^{a}	3.54 ± 0.09^{a}
AST (IU L^{-1})	201.2 ± 7.2	154 ± 9.6	176 ± 10.7
ALP (IU L^{-1})	454.4 ± 19.4	209.2 ± 14.2	482.8 ± 24.5
ALT (IU L^{-1})	79.1 ± 4.62	40.9 ± 2.93	55 ± 1.64
LDH (IU L^{-1})	2921 ± 91.27	2915 ± 184.6	3425 ± 81.5
BUN (mg/dL)	104.5 ± 3.74	80.7 ± 4.41	130.4 ± 6.47

Different letters indicate significant differences in rows ($p < 0.05$)

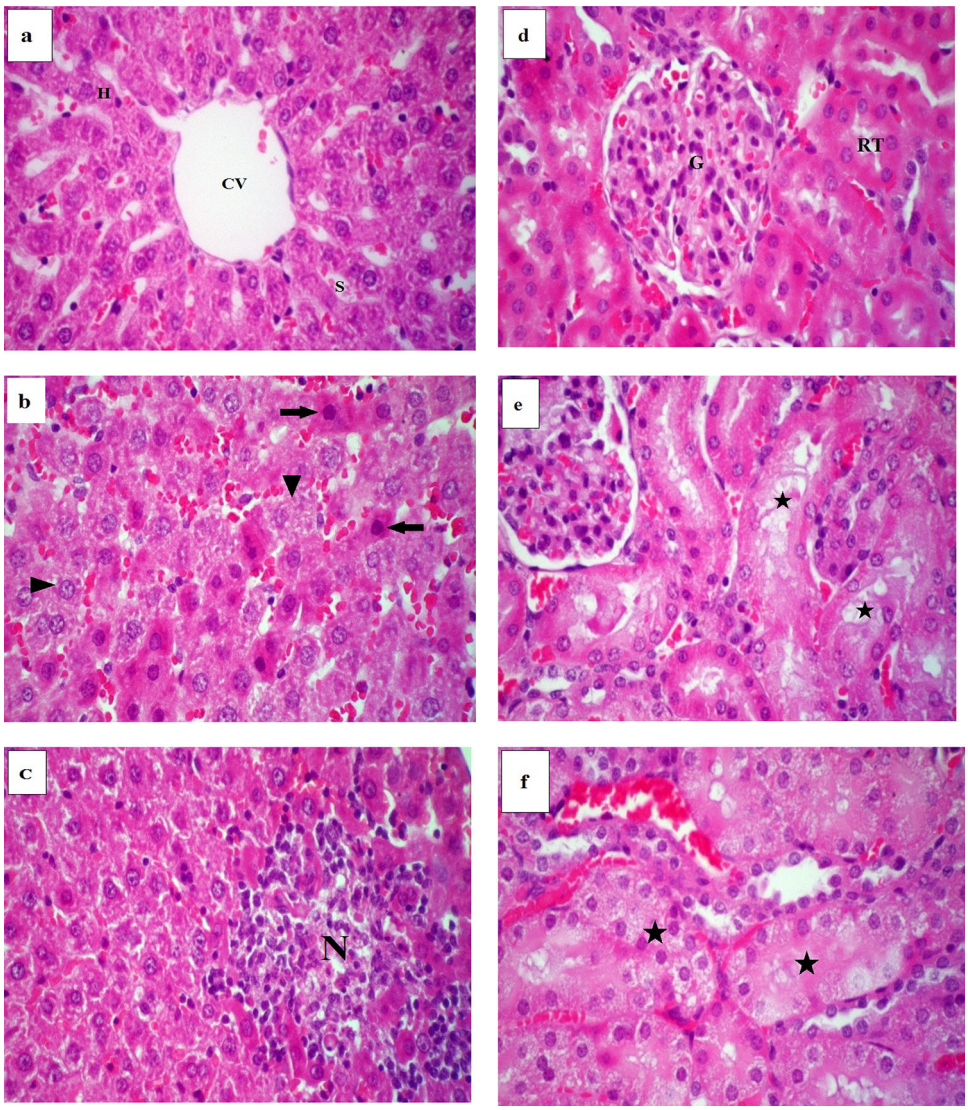

Fig. 7 Photomicrographs of the liver and kidney tissues in the rats treated with SiO_2 and MgO NPs (H&E, × 400). **a** Control group, liver parenchyma with normal histological architecture of hepatic cells (**h**), central vein (CV) and sinusoids (S). **b** 2000 mg/kg MgO NPs group, showing hepatocellular swelling and degeneration (arrowheads), and individual cell necrosis with significant pyknotic nuclei and eosinophilic cytoplasm (arrows). **c** 2000 mg/kg of SiO_2 group, liver parenchyma with focal hepatocellular necrosis and mononuclear inflammatory cells infiltration (N). **d** Control group, kidney with normal histological structure of glomerular tuft (**g**) and renal tubules (RT). **e** 2000 mg/kg MgO NPs group, showing mild to moderate renal tubular epithelial cell swelling and hydropic degeneration (asterisks). **f** 2000 mg/kg of SiO_2 group, kidney tissue with renal tubular epithelial cell swelling, degeneration (asterisks), and vascular congestion

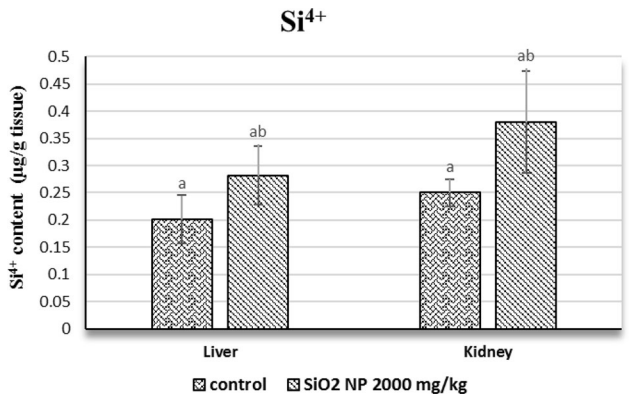

Fig. 8 Si^{+4} concentrations were determined in the liver and kidney tissues by ICP-OES after the digestion with nitric acid and perchloric acid

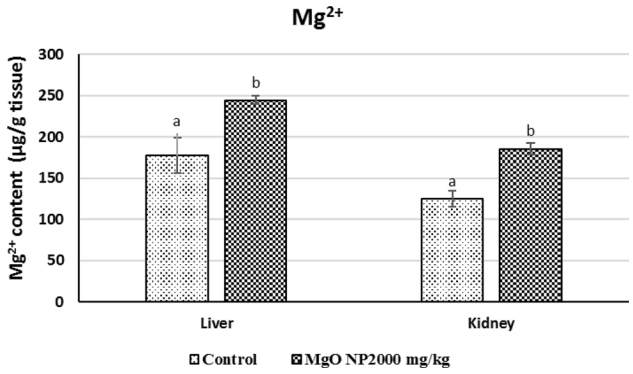

Fig. 9 Mg^{2+} concentrations were determined in the liver and kidney tissues by AAS after the digestion with nitric acid and perchloric acid

The biochemical results of the present study showed that the acute doses of MgO NPs decreased the serum activity of AST and ALT at the end of the study. AST and ALT have a clearance half-life of approximately 12 h and 60 h in dogs, respectively (Latimer 2011). It seems that, at first, the serum activity of these hepatic enzymes may increase due to the acute hepatocellular degeneration and necrosis, but due to the complete evacuation of enzymes and their short half-life in the serum, the activity of these enzymes decreased after 14 days (Latimer 2011). Moreover, 2000 mg/kg MgO NPs induced a significant decrease in the serum ALP activity of the treated rats compared to the control group. ALP is a specific enzyme for cholestasis. Increased serum ALP activity results from enzyme induction, typically happening as a consequence of cholestasis, drug or hormonal effects (Latimer 2011). AST and LDH are not liver-specific; they are found in most tissues. A significant change in serum AST and LDH activity may occur after liver, heart, or muscle injury (Latimer 2011). In contrast, the results indicated no significant difference in the serum LDH and AST between the treated groups with SiO_2 NPs and the control. It shows that SiO_2 NPs had no tissue injury in 2000 mg/kg dosage. Sulaiman et al. (2015) indicated that the reduction in AST and ALP activities caused by the nanoparticle may be due to inactivation arising from the affinity of the Ag nanoparticles for thiol (eSH) groups, thereby causing change in the functional state of proteins.

Our findings are not in line with those of some other researchers. In a previous study, the biochemical examination of rats after their exposure to 1000 mg/kg BW MgO NPs revealed that LDH, AST, and ALT activities increased in serum. Moreover, the authors of that study reported that serum biochemical markers, such as albumin, calcium, glucose, chloride, cholesterol, HDL, triglycerides, and creatinine, were significant at high doses of NP administered to a group of rats (Mangalampalli et al. 2017). Mazaheri's study results showed that injection of high concentrations of magnesium oxide nanoparticles (250 and 500 µg/mL) significantly increased AST and ALP. But didn't alter ALT, GGT, urea, and creatinine levels (Mazaheri et al. 2019). In another study, Wang et al. (2006) evaluated the acute toxicity study of the oral exposure to zinc (Zi) nanoscale in mice. Their results showed that Zi NPs elevated the level of ALT, AST, ALP, and LDH in the M-Zn- and N-Zn-treated rats (Wang et al. 2006). Sharma et al. (2012) reported that ZnO NPs at a dose of 300 mg/kg significantly increased the activity of ALT and ALP in the treated mice compared to the control mice (Sharma et al. 2012). Hassankhani et al. (2015) showed that the toxicity of orally administrated SiO_2 NPs in adult mice induced a significant increase in serum AST, LDH, and ALT activity (Hassankhani et al. 2015). Mazaheri et al. (2019) indicated that high concentrations of magnesium oxide nanoparticles (250 and 500 µg/mL) significantly elevated white blood cells, red blood cells, hemoglobin, and hematocrit compared with the control group. Moreover, their results showed that the nanoparticles elevated the levels of AST and ALP, whereas there was no significant change in levels of ALT, GGT, urea, and creatinine for the dose of particles (Mazaheri et al. 2019).

The current study's findings were partly similar to those of Chan et al. (2017), who demonstrated that the levels of serum AST and ALT activity did not increase significantly. In addition, total bilirubin, total protein, and albumin were similar to the control. Their results also showed that BUN and creatinine did not increase after the injection of SiO_2 NPs (Chan et al. 2017). Furthermore, Yu et al. (2013) evaluated the acute toxicity of intravenously administrated amorphous SiO_2 NPs in mice. Their biochemical results showed that the serum LDH, AST, and ALT activity increased in the SiO_2 NP-treated groups (Yu et al. 2013).

The results indicated a significant difference in the concentration of BUN at a high dose of MgO NPs (2000 mg/kg) administrated to a group of rats. Decreased

BUN concentration may be due to the reduced conversion of ammonia to urea and the reduction of urea synthesis because of hepatic injury and disease.

There was no significant difference between the control and other groups in terms of triglyceride and cholesterol. This shows that MgO and SiO_2 NPs poisoning did not affect blood lipids. The serum glucose level decreased in 2000 mg/kg MgO NPs groups compared with the control group. This reduction probably was due to the glucose consumption by tissue cells that could cause a decrease in blood. However, in 2000 mg/kg SiO_2 NPs groups, the glucose level increased, showing the due stress of poisoning.

The 2000 mg/kg doses of MgO and SiO_2 NPs significantly decreased serum Ca level. In addition, phosphorus showed a significant reduction at 2000 mg/kg SiO_2 NPs doses. The reduction in Ca level in SiO_2 and MgO groups could be attributed to some digestive disorders such as malabsorption or poisoning. Acute poisoning and gastrointestinal diseases have been reported to cause a decrease in the Ca level (Latimer 2011). Perhaps, the reason for such decrease is malabsorption, which, on the one hand, reduces Ca and, on the other hand, reduces phosphorus by, for example, reducing the absorption of calcium and vitamin D in the intestines.

In the current study, the results indicated that the oral administration of 2000 mg/kg MgO NPs and SiO_2 NPs in rats did not cause any adverse pathological changes at the end of the study period, which lasted 14 days. However, the histopathological analysis of the rats treated with MgO NPs at a dose of 2000 mg/kg revealed the presence of mild congestion, non-zonal hepatocellular swelling and degeneration, and necrotic cells with significant pyknotic or shrunken nuclei. Also, the histopathologic examination of the kidney tissue sections showed mild congestion and hemorrhage, irregularly renal tubular epithelial cell swelling, and cytoplasmic degeneration in Henle's convoluted tubules and loops without any nuclear, interstitial inflammation, and/or proliferative changes. Moreover, the histopathological analysis of the heart, lungs, and spleen revealed no microscopic abnormalities in both NPs and dosages in the treated rats compared to the control. These findings agree with those of another study done by Mangalampalli et al. (2017). They investigated the effects of the oral administration of different doses of MgO NPs on rats for 14 days and did not observe any adverse pathological changes during the study period. Their results showed that MgO NPs at a dose of 2000 mg/kg induced spaces between hepatocytes and tissue degeneration in the liver and swelling in the renal glomerulus in the kidney. Also, they did not observe any morphological changes in the heart, brain, and spleen of the treated rats compared to those in the control group. Mazaheri et al. (2019) reported that the MgO nanoparticles-treated rats demonstrated some changes, including proliferation of bile ductules, sinusoids, and congestion, in the liver mainly at the highest concentration. They observed that the MgO nanoparticles-treated kidney with various doses did not exhibit degenerative effects in the cells (Mazaheri et al. 2019).

In the current study, and under the microscopic examination, the histological assessment of the liver of the treated rats with 2000 mg/kg of SiO_2 NPs demonstrated focal hepatocellular degeneration, necrosis, accumulation of mononuclear inflammatory cells within the necrotic area, sinusoidal congestion, and focal edematous fluids in the hepatic parenchyma. Furthermore, minimal to mild random tubular epithelial cell swelling and degeneration, and renal congestion were observed in the kidneys of rats treated at 2000 mg/kg dosage of Si NPs.

In recent studies, no apparent histopathological abnormalities or lesions have been reported. Nevertheless, lymphocytic infiltration and swelling in the liver have been observed in the treated rats with 240 mg/kg BW of SiO_2 NPs. Some researchers reported that after the intravenous injection of SiO_2 NPs into the mice, no toxic effects were observed at low doses, while a high dose of SiO_2 NPs damaged their liver (Fu et al. 2012). A study by Yu et al. (2013) demonstrated that SiO_2 NPs could lead to lymphocytic infiltration, granuloma formation, and hydropic degeneration in the liver's hepatocytes (Yu et al. 2013).

In the present study, as confirmed by ICP-OES and AAS analysis, a significant biodistribution of MgO NPs occurred in the liver and kidney of the treated rats. Also, a small amount of SiO_2 NPs was penetrated the liver. This finding was similar to that of FU et al. (2013). They reported that the body absorbed NPs with 110 nm at 24 h after the oral administration. Furthermore, they said that the liver was the target organ after intravenous, oral, and hypodermic administration.

5 Conclusion

According to the current study results, it can be concluded that MgO and SiO_2 NPs can be absorbed through the gastrointestinal tract into the bloodstream and accumulate in the liver and kidney of rats. In addition, the biochemical parameters and histopathological findings indicated that MgO and SiO_2 NPs could cause changes in the kidney and liver tissues and liver enzymes. The present study's findings show that these NPs at high concentrations can have toxicological effects on the liver and kidneys of rats. These results indicate that the safety of the NPs and the evaluation of their toxic effects are crucial issues that should be addressed before NPs are allowed to enter the consumer market.

Acknowledgements We would like to thank Ms. M. Aghazi, Mr. Y Khosravi, Dr. S Zeinali, Dr. F. Zarei, and Mr. H. A. Shamsaei for their technical assistance.

Funding Shahrekord University and Shiraz University financially supported this research, Ministry of Science, Research, and Technology, Iran.

Declarations

Conflict of Interest The authors declare that they have no conflict of interest.

References

Chan WT, Liu CC, Chiau JS, Tsai ST, Liang CK, Cheng ML, Lee HC, Yeung CY, Hou SY (2017) In vivo toxicologic study of larger silica nanoparticles in mice. Int J Nanomed 12:3421. https://doi.org/10.2147/IJN.S126823

Cho M, Cho WS, Choi M, Kim SJ, Han BS, Kim SH, Kim HO, Sheen YY, Jeong J (2009) The impact of size on tissue distribution and elimination by single intravenous injection of silica nanoparticles. Toxicol Lett 189(3):177–183. https://doi.org/10.1016/j.toxlet.2009.04.017

Dhal JP, Sethi M, Mishra BG, Hota G (2015) MgO nanomaterials with different morphologies and their sorption capacity for removal of toxic dyes. Mater Lett 15(141):267–271. https://doi.org/10.1016/j.matlet.2014.10.055

Ding T, Yao L, Liu C (2016) Kinetically-controlled synthesis of ultra-small silica nanoparticles and ultra-thin coatings. Nanoscale 8(8):4623–4627. https://doi.org/10.1039/C5NR08224B

Dummer NF, Joyce L, Ellicott H, Jiang Y (2016) Surfactant controlled magnesium oxide synthesis for base catalysis. Catal Sci Technol 6(6):1903–1912. https://doi.org/10.1039/C5CY01107H

Fu C, Liu T, Tang F, Chen D, Li L, Liu H, Li X (2012) Acute toxicity and oxidative damage induced by silica nanorattle in vivo. Chin Sci Bull 57(20):2525–2532. https://doi.org/10.1007/s11434-012-5187-y

Fu C, Liu T, Li L, Liu H, Chen D, Tang F (2013) The absorption, distribution, excretion and toxicity of mesoporous silica nanoparticles in mice following different exposure routes. Biomaterials 34(10):2565–2575. https://doi.org/10.1016/j.biomaterials.2012.12.043

Gelli K, Porika M, Anreddy RN (2015) Assessment of pulmonary toxicity of MgO nanoparticles in rats. Environ Toxicol 30(3):308–314. https://doi.org/10.1002/tox.21908

Ghobadian M, Nabiuni M, Parivar K, Fathi M, Pazooki J (2017) Histopathological evaluation of zebrafish (*Danio rerio*) larvae following embryonic exposure to MgO nanoparticles. IJFS 16(3):959–969

Go MR, Bae SH, Kim HJ, Yu J, Choi SJ (2017) Interactions between food additive silica nanoparticles and food matrices. Front Microbiol 8:1013. https://doi.org/10.3389/fmicb.2017.01013

Hassankhani R, Esmaeillou M, Tehrani AA, Nasirzadeh K, Khadir F, Maadi H (2015) In vivo toxicity of orally administrated silicon dioxide nanoparticles in healthy adult mice. Environ Sci Pollut Res Int 22(2):1127–1132. https://doi.org/10.1007/s11356-014-3413-7

Hochella MF Jr, Lower SK, Maurice PA, Penn RL, Sahai N, Sparks DL, Twining BS (2008) Nanominerals, mineral nanoparticles, and earth systems. Science 319(5870):1631–1635

Ivask A, Voelcker NH, Seabrook SA, Hor M, Kirby JK, Fenech M, Davis TP, Ke PC (2015) DNA melting and genotoxicity induced by silver nanoparticles and graphene. Chem Res Toxicol 28(5):1023–1035. https://doi.org/10.1021/acs.chemrestox.5b00052

Kim YR, Lee SY, Lee EJ, Park SH, Seong NW, Seo HS, Shin SS, Kim SJ, Meang EH, Park MK, Kim MS (2014) Toxicity of colloidal silica nanoparticles administered orally for 90 days in rats. Int J Nanomedicine 9(Suppl 2):67–78. https://doi.org/10.2147/IJN.S57925

Krishnamoorthy K, Moon JY, Hyun HB, Cho SK, Kim SJ (2012) Mechanistic investigation on the toxicity of MgO nanoparticles toward cancer cells. J Mater Chem 22(47):24610–24617. https://doi.org/10.1039/C2JM35087D

Latimer KS (2011) Duncan and Prasse's veterinary laboratory medicine, clinical pathology book, 5th edn. Wiley-Blackwell, New York

Mangalampalli B, Dumala N, Grover P (2017) Acute oral toxicity study of magnesium oxide nanoparticles and microparticles in female albino Wistar rats. Regul Toxicol Pharmacol 1(90):170–184. https://doi.org/10.1016/j.yrtph.2017.09.005

Martinez-Boubeta C, Balcells L, Cristòfol R, Sanfeliu C, Rodríguez E, Weissleder R, Lope-Piedrafita S, Simeonidis K, Angelakeris M, Sandiumenge F, Calleja A (2010) Self-assembled multifunctional Fe/MgO nanospheres for magnetic resonance imaging and hyperthermia. Nanomed Nanotechnol Biol Med 6(2):362–370. https://doi.org/10.1016/j.nano.2009.09.003

Mazaheri N, Naghsh N, Karimi A, Salavati H (2019) In vivo toxicity investigation of magnesium oxide nanoparticles in rat for environmental and biomedical applications. Iran J Biotechnol 17(1):1–9. https://doi.org/10.21859/IJB.1543

Morishita Y, Yoshioka Y, Satoh H, Nojiri N, Nagano K, Abe Y, Kamada H, Tsunoda SI, Nabeshi H, Yoshikawa T, Tsutsumi Y (2012) Distribution and histologic effects of intravenously administered amorphous nanosilica particles in the testes of mice. Biochem Biophy Res Commun 420(2):297–301. https://doi.org/10.1016/j.bbrc.2012.02.153

Nishimori H, Kondoh M, Isoda K, Tsunoda SI, Tsutsumi Y, Yagi K (2009) Histological analysis of 70-nm silica particles-induced chronic toxicity in mice. Eur J Pharm Biopharm 72(3):626–629. https://doi.org/10.1016/j.ejpb.2009.03.007

Park SB, Jung WH, Kim KY, Koh B (2020) Toxicity assessment of SiO_2 and TiO_2 in normal colon cells, in vivo and in human colon organoids. Molecules 25(16):3594. https://doi.org/10.3390/molecules25163594

Purwajanti S, Zhou L, Ahmad Nor Y, Zhang J, Zhang H, Huang X, Yu C (2015) Synthesis of magnesium oxide hierarchical microspheres: a dual-functional material for water remediation. ACS Appl Mater Interfaces 7(38):21278–21286. https://doi.org/10.1021/acsami.5b05553

Sahoo SK, Parveen S, Panda JJ (2007) The present and future of nanotechnology in human health care. Nanomed: Nanotechnol Biol Med 3(1):20–31. https://doi.org/10.1016/j.nano.2006.11.008

SCENIHR (Scientific Committee on Emerging and Newly-Identified Health Risks) (2007) Opinion on the scientific aspects of the existing and proposed definitions relating to products of nanoscience and nanotechnologies. 29 November 2007, the existing and proposed definitions relating to products of nanotechnologies

Sharma V, Singh P, Pandey AK, Dhawan A (2012) Induction of oxidative stress, DNA damage and apoptosis in mouse liver after sub-acute oral exposure to zinc oxide nanoparticles. Mutat Res/genet Toxicol Environ Mutagen 745(1–2):84–91. https://doi.org/10.1016/j.mrgentox.2011.12.009

Sulaiman FA, Adeyemi OS, Akanji MA, Oloyede HOB, Sulaiman AA, Olatunde A, Hoseni AA, Olowolafe YV, Nlebedim RN, Muritala H, Nafiu MO, Salawu MO (2015) Biochemical and morphological alterations caused by silver nanoparticles in Wistar rats. J Acute Med 5(4):96–102

Van Der Zande M, Vandebriel RJ, Groot MJ, Kramer E, Herrera Rivera ZE, Rasmussen K, Ossenkoppele JS, Tromp P, Gremmer ER, Peters RJ, Hendriksen PJ (2014) Sub-chronic toxicity study in rats orally exposed to nanostructured silica. Part Fibre Toxicol 11(1):1–9. https://doi.org/10.1186/1743-8977-11-8

Wang B, Feng WY, Wang TC, Jia G, Wang M, Shi JW, Zhang F, Zhao YL, Chai ZF (2006) Acute toxicity of nano-and micro-scale zinc powder in healthy adult mice. Toxicol Lett 161(2):115–123. https://doi.org/10.1016/j.toxlet.2005.08.007

Yu T, Greish K, McGill LD, Ray A, Ghandehari H (2012) Influence of geometry, porosity, and surface characteristics of silica nanoparticles on acute toxicity: their vasculature effect and tolerance threshold. ACS Nano 6(3):2289–2301. https://doi.org/10.1021/nn2043803

Yu Y, Li Y, Wang W, Jin M, Du Z, Li Y, Duan J, Yu Y, Sun Z (2013) Acute toxicity of amorphous silica nanoparticles in intravenously exposed ICR mice. PLoS ONE 8(4):e61346. https://doi.org/10.1371/journal.pone.0061346

Zhang H, Ji Z, Xia T, Meng H, Low-Kam C, Liu R, Pokhrel S, Lin S, Wang X, Liao YP, Wang M (2012) Use of metal oxide nanoparticle band gap to develop a predictive paradigm for oxidative stress and acute pulmonary inflammation. ACS Nano 6(5):4349–4368. https://doi.org/10.1021/nn3010087